Wood Sci Technol (2007) 41:551–564
DOI 10.1007/s00226-007-0132-y

ORIGINAL

Three-dimensional imaging of a sawn surface: a comparison of confocal microscopy, scanning electron microscopy, and light microscopy combined with serial sectioning

Lloyd Donaldson · Stig Bardage · Geoffrey Daniel

Received: 7 November 2006 / Published online: 5 May 2007

Abstract The three-dimensional structure of a transverse sawn wood surface was investigated using several methods, to compare techniques, and to study the types of deformation in tracheids at the saw cut. A sample of spruce sapwood was cut with a fret saw across the grain. The transverse sawn surface was imaged by confocal microscopy, field emission scanning electron microscopy (FESEM), and by light microscopy combined with serial sectioning and three-dimensional (3D) reconstruction. Both confocal microscopy and FESEM were restricted to visualising the cut surface of the wood. However, serial sectioning was able to reveal the internal structure below the cut surface providing more information on the types of cell deformation present. The wood structure was deformed to depths of more than 600 μm below the surface with twisting, crushing and tearing deformations. Near the outer surface, gaps were formed between groups of tracheids where the cell walls had been torn away to form saw dust. The deformation tended to form groups of tracheids that were twisted relative to each other. Latewood was less distorted, forming a dense solid surface compared to the highly fibrous earlywood.

Introduction

Most studies examining the microscopic structure of wood surfaces prepared by industrial processing such as sawing, planing and sanding, have been undertaken in relation to coating and adhesive performance. The microstructure of machined

L. Donaldson (✉)
Cellwall Biotechnology Centre, Scion, Private Bag 3020, Rotorua, New Zealand
e-mail: lloyd.donaldson@scionresearch.com

S. Bardage · G. Daniel
Wood Ultrastructure Research Centre, Swedish University of Agricultural Science, Uppsala, Sweden

end-grain surfaces of spruce timber has been examined using scanning electron microscopy (SEM) in an effort to understand problems with end-grain joining (Nordström 1995; Nordström and Johansson 1995). The surface was described as very deformed or demolished to depths of 100–200 μm as a result of either sawing or planing. No change was found in the depth of demolition between sawing and planing, or when the direction of machining was altered. The crushed surface was dense and compact especially in latewood regions, and was considered to be an effective barrier to adhesives and coatings. Contamination of the surface with extractives from the crushed resin canals was also considered to contribute to joining or coating problems.

Suchsland (1958) found that adhesive penetration was restricted to earlywood of end-grain surfaces while Marian et al. (1958) found that the strength of end-grain joints increased with surface roughness to a certain level before subsequently declining again. The decrease was due to increasing fibre damage which increased with decreasing density. Sawn surfaces that are free from cell debris have improved end-grain joint strength because there are fewer damaged fibres producing a more porous surface for penetration of adhesive compared with a sanded end-grain surface (Bassett 1960). Quirk et al. (1967) found that difference in the tensile strength of earlywood and latewood end-grain joints was related to cell lumen size and the ability of the surface to absorb adhesive to provide continuity between the solid undamaged wood below the sawn surface, and the adhesive film at the joint.

Several studies have examined defect formation on planed surfaces at the micro level. Stehr and Östlund (2000) investigated crack formation on planed longitudinal wood surfaces of pine and found that cracks form at earlywood/latewood boundaries exposed at the planed surface. They found that such cracks are more likely to form on the pith side than the bark side after machining operations. The microstructure of sanded and polished wood surfaces from pine and spruce has been studied by replication of the surface comparing the radial, tangential and cross sectional surfaces (Wu 1998). This technique was aimed more as a preparation method for microscopy than as an investigation of the effect of machining on cell walls. Liptakova et al. (1995) briefly examined the structure of sanded or milled wood surfaces and found that crushed cell walls are pressed into the surface pores resulting in a loss of surface roughness.

The structure of tangential sanded wood surfaces has been examined by scanning electron microscopy with evidence for tearing and crushing of cells both at the surface, and up to 50–80 μm below the surface (Stewart and Crist 1982; Murmanis et al. 1986; de Moura and Hernández 2006). The layer of damaged cells reduces the penetration of coatings into the wood (de Meijer et al. 1998), and may produce a mechanically weak boundary layer at the glueline in adhesive joints (Hernández and Rojas 2002; de Moura and Hernández 2005). Planing may produce similar damage at depths of up to 65–100 μm (Hernández and Rojas 2002).

Singh and Dawson (2006) examined the wood coating interface of saw-textured plywood using a range of microscopy techniques including light microscopy, confocal microscopy and scanning electron microscopy. They found that the surface tissues were greatly distorted with the applied coating closely conforming to the contours of the surface texture to produce a film of variable thickness. Scanning

electron microscopy was used to evaluate the surfaces produced by different saw tooth types in normal and tension wood of maple (Vazquez-Cooz and Meyer 2006) indicating that fuzzy grain in tension wood is responsible for increased power consumption by causing friction against the machining tool.

Three-dimensional imaging of wood structure and wood based products has been carried out using a number of techniques. Confocal microscopy has been used for 3D reconstruction of developing xylem (Kitin et al. 2003; Möller et al. 2003), paper fibres (Jang et al. 1991, 1995) and wood structure in a range of species (Donaldson and Bond 2005). Serial sectioning combined with light microscopy or scanning electron microscopy has also been used to construct virtual models of paper structure (Chinga et al. 2004), individual spruce tracheids (Bardage 2001), and pulp fibres (Bardage et al. 2002).

We have applied a range of imaging techniques including confocal microscopy, scanning electron microscopy, and serial sectioning combined with conventional light microscopy, followed by 3D reconstruction, to investigate the deformation of tracheids on a transversely sawn surface of spruce wood.

Materials and methods

Green spruce (*Picea abies* L.) sapwood sampled at ring 16 from the pith at breast height (30 growth rings at breast height, diameter 174 mm) was prepared by sawing across the grain using a fret saw. The sample was divided into a number of smaller blocks and prepared for microscopy as follows.

Confocal microscopy

A small block incorporating the transverse sawn surface was saturated in water, stained with safranine (0.1% aq.) for 5 min and washed extensively in water. The block was air dried, mounted on a microscope slide, and the sawn surface was covered with immersion oil and a coverslip. The sample was examined by confocal microscopy using a Leica TCS/NT confocal microscope. Excitation wavelength was 568 nm and emission wavelength was 600+ nm. A series of optical sections were acquired at 1 μm intervals over a depth of approximately 80 μm, and projected as anaglyphs for stereoscopic viewing, or as maximum intensity projections (a method for rendering surfaces). Different perspective views were generated by rotating the point of view using Digital Optics V++ software to make projection series.

Electron microscopy

A small air-dried block including the sawn surface was mounted on an aluminium stub using colloidal silver adhesive and coated with a thin layer of chromium in a sputter coater. The sample was examined using a JEOL 6700F field emission scanning electron microscope (FESEM) at an accelerating voltage of 500 V. Stereoscopic images were made by taking two images of each field of view with eucentric stage rotation using a 4° difference in tilt. Images were then overlaid to create an anaglyph for stereoscopic viewing.

Serial sectioning and light microscopy

Several $2 \times 2 \times 2$ mm^3 blocks were prepared from the sawn surface, dehydrated in an acetone series and embedded in Spurr's resin. Blocks were sectioned using glass knives on an LKB ultramicrotome at 2 μm intervals in series from the outer part of the sawn surface until undeformed wood could be detected. One complete sequence was prepared after several practice runs. Sections were stained with safranine, mounted in immersion oil and imaged using brightfield light microscopy. Images of each section were acquired using a CCD camera. Sections were roughly oriented on the microscope but digital images were subsequently precisely oriented by rotation and translation using Digital Optics V++ software. It was possible to orient the images adequately without the use of fiducial marks by using landmark features of the preceding image for alignment. Individual images showed varying amounts of stretching but this was small enough that no correction was necessary. Aligned stacks of images were binarised using an average brightness threshold (Moëll and Donaldson 2001), depth shaded (one grey level per 2 μm interval) and projected as anaglyph images for stereoscopic viewing, or as depth shaded projections (deeper slices are darker), using Digital Optics V++ software. Because of the very complex internal structure of the sawn surface, the volume was divided into three smaller sequences representing 0–300, 300–500 and 500–635 μm below the surface, and these were projected separately. Some surface rendering was also attempted using the procedure described by Bardage (2001) using non-uniform rational b-splines (NURBS).

Results

Confocal microscopy

Confocal microscopy using safranine staining produced detailed images of tracheid distortion and damage but images were largely restricted to the outer surface (Fig. 1). Because tracheids are folded and compressed to form a dense light-absorbing surface it was not possible to image the internal structure of the sawn surface (Fig. 1). Cell walls are good light absorbers (Donaldson and Lausberg 1998) and this is apparently enhanced by the densification at the outer margin of the sawn surface. Individual tracheids had torn edges and were compressed into flaps of double cell wall that were then folded across each other horizontally (Fig. 1). Small cell wall fragments filled the spaces between the folded flaps making a dense compact surface. Earlywood was highly fibrous with the amount of roughness varying from place to place.

Electron microscopy

The very rough structure of the sawn surface would be expected to cause some problems for conventional scanning electron microscopy because of charging effects due to non-uniform conduction in different parts of the rough surface. To

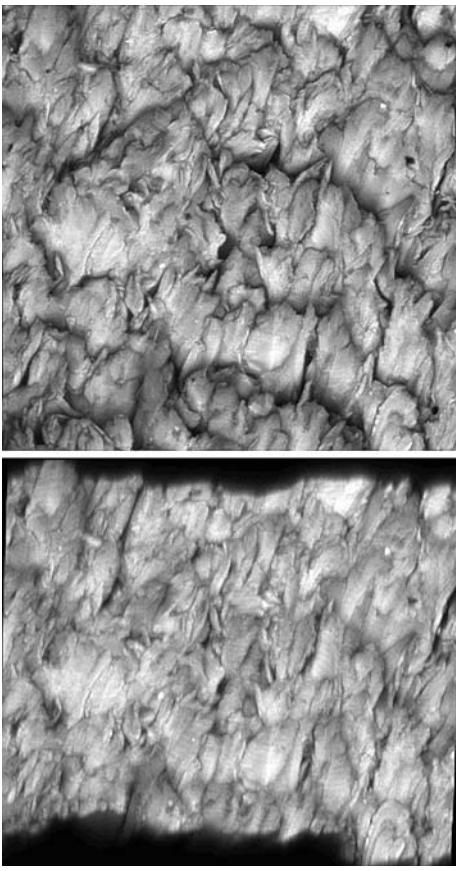

Fig. 1 Confocal fluorescence image (maximum intensity projection) of a sawn surface at 0° (*top*) and 45° (*bottom*) tilt showing torn, compressed, and folded tracheids at the surface of an earlywood region. Field of view 625 × 625 μm

overcome this problem a very low accelerating voltage of only 500 V was used. Comparison of image quality over a range of accelerating voltages indicated that charging effects were significant from 600 to 3 kV and above but were more or less eliminated at 500 V. FESEM produced similar images to confocal microscopy but allowed visualisation of larger areas (Fig. 2). Imaging of the internal structure of the sawn surface was restricted to cut edges of the block making the internal structure difficult to visualise (Fig. 2). The direction of tracheid distortion varied across the surface probably corresponding to the alternating direction of the saw blade during cutting.

Earlywood surfaces show extensive deformation of tracheids (Fig. 2), which have irregular torn ends. The tracheids are highly compressed forming flat sheets of cell wall that are either bent over or partially erect. Adjacent tracheids are oriented in similar directions but groups of tracheids have varying orientations at different locations across the sawn surface. In contrast, latewood has a dense featureless

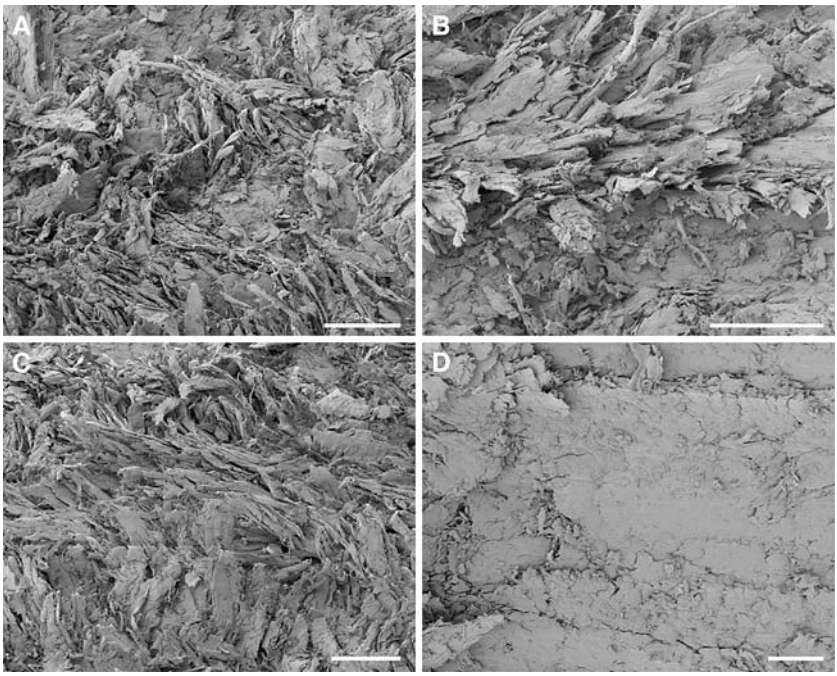

Fig. 2 A range of scanning electron micrographs illustrating the severe distortion of tracheids at the sawn surface. Earlywood surfaces (**a**–**c**) are fibrous with torn and compressed tracheids projecting from the surface in varying orientations. In contrast, the latewood surface (**d**) is dense and compact with few recognisable anatomical features. *Scale bar* 100 μm

surface with few if any recognisable anatomical features (Fig. 2). Latewood tracheid cell walls appear to have fused into a solid mass, probably by folding of torn tracheid cell walls across the lumens. As with confocal microscopy, scanning electron microscopy only reveals surface details except for limited views of deformed tracheids visible on cut radial longitudinal surfaces.

Serial sectioning

Serial sectioning was the most time consuming of the three techniques used, taking several weeks to complete the sectioning and imaging, followed by several days to align the stack of images. However in comparison to confocal imaging and FESEM, serial sectioning did allow clear visualisation of the internal structure of the sawn surface (Figs. 3, 4, 5). Three-dimensional reconstruction was completed for three separate parts of the volume because projecting the entire volume did not clearly illustrate the complex internal structure of the sawn surface. In addition to projection of the volume it was also possible to examine individual sections at known depths as shown in Fig. 3.

In the outer 300 μm, tracheids were distributed in groups surrounded by empty spaces where cell walls had been torn away during sawing to form sawdust

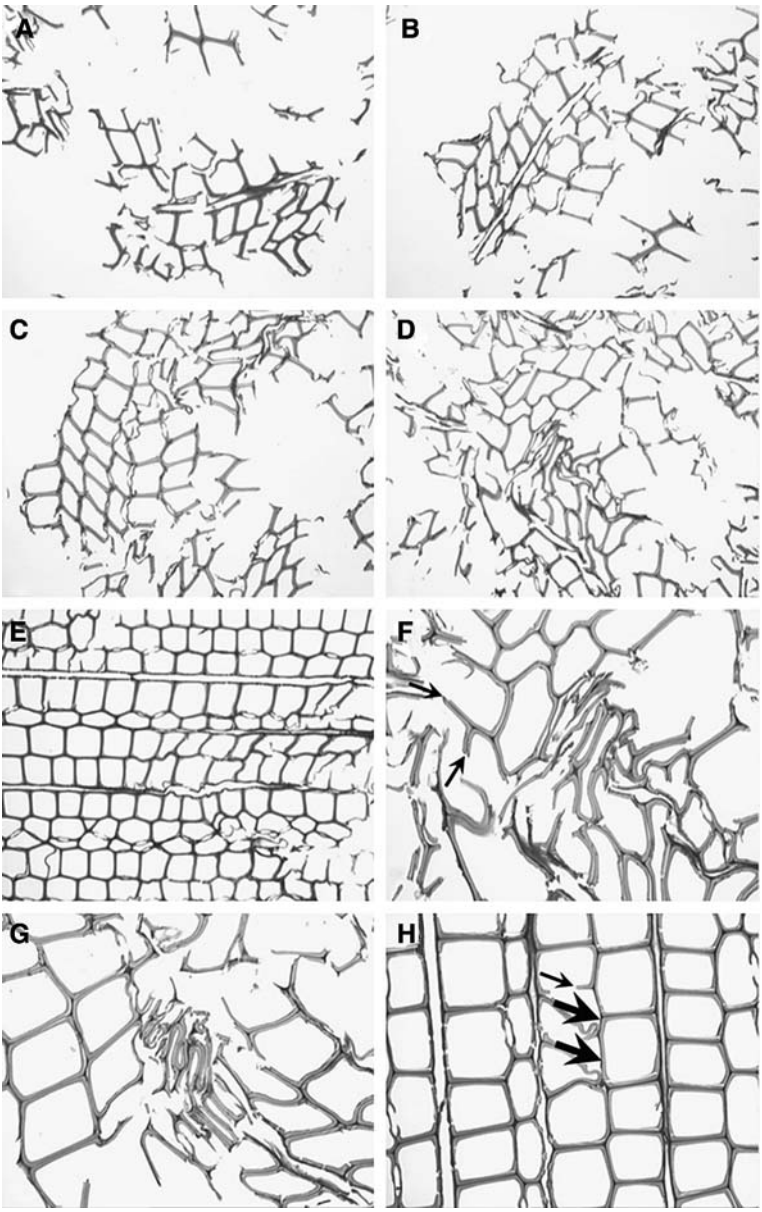

Fig. 3 A series of individual sections using conventional light microscopy, illustrating the cell deformation at different depths within the sawn surface. The images from *top left* (**a**–**e**) are at 110, 140, 220, 314 and 620 μm depth, respectively. The higher magnification images (**f**–**h**) show examples of compression, and collapse with combined trans-wall (*small arrows*) and intra-wall (*large arrows*) fracture. Field of view is 450 μm wide for **a**–**e** and 225 μm for **f**–**h**

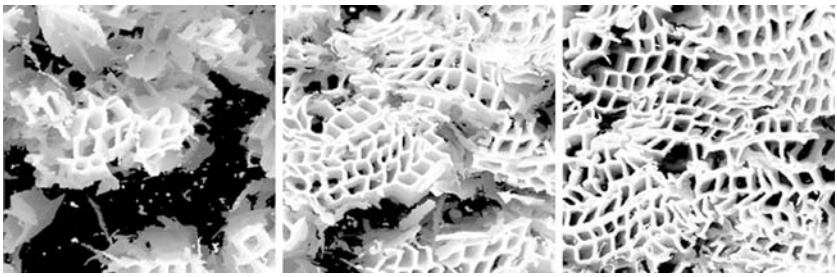

Fig. 4 Depth shaded maximum intensity projections based on light microscopy of serial sections showing three-dimensional reconstruction of successive depths below the sawn surface from 0–300, 300–500 to 500–635 μm from *left* to *right*. Field of view 625 × 625 μm

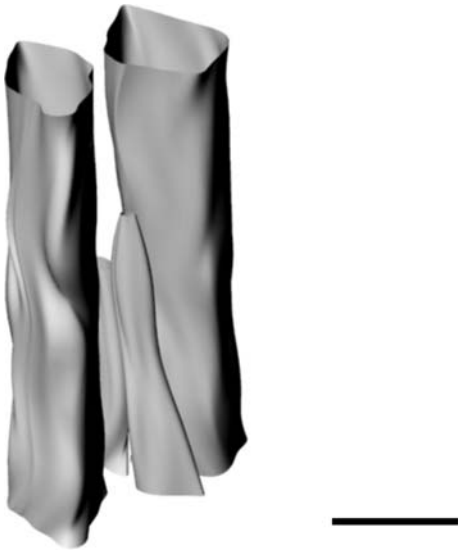

Fig. 5 Surface rendered view of tracheid lumen outlines in deformed tracheids based on light microscopy of serial sections. *Scale bar* 30 μm

(Figs. 3, 4, 5). Individual groups of tracheids were twisted (Fig. 5) and crushed with tracheids at the margins and towards the surface of each group having torn and shredded cell walls, often with cell wall fragments extending out into the empty regions (Figs. 3, 4). Tracheids in the centre of these groups were less damaged and only slightly compressed. These internal features, including grouping of tracheids and the variable deformation, were not apparent by either confocal microscopy or scanning electron microscopy and thus represent new information.

In the middle zone from 300–500 μm below the surface, empty spaces were smaller and the tracheid groups were correspondingly larger but the distortion was similar to that described for the outer zone (Figs. 3, 4). In the inner zone from 500 to 635 μm the wood structure gradually became less distorted with increasing depth.

The groups of tracheids were surrounded on their margins by crushed or torn cells, the more interior cells still showing significant twisting. Beyond 635 μm from the surface there were significant areas of un-deformed tracheids, with only occasional crushed or otherwise damaged tracheids (Fig. 3). While the quality of 3D reconstruction is limited to some extent by the accuracy of alignment, the projections are remarkably informative and clearly show the cell wall damage in an extended view not possible by examining individual sections (Figs. 4, 5).

Examination of individual sections reveals some details of the type of cell wall damage caused by the sawing (Fig. 3). Tracheids at the perimeter of the bundles have torn cell walls so that the lumen is exposed by trans- and intra-wall fracture. The tracheids in the interior of the bundle are deformed by mild crushing and twisting but most lumens are open. At depths beyond 300 μm some adjacent bundles come into contact and are attached to each other by severely crushed tracheids that may extend well into less deformed regions (Fig. 3f, g). Both trans- and intra-wall fractures are common, resulting in tracheids with large holes in their cell walls. Some tracheids may be detached from each other adjacent to the middle lamella (Fig. 3h).

Stereo imaging

Stereo imaging can be applied to all three techniques used in this study to reveal the 3D structure more clearly. The 3D texture of the surface with projecting tracheids and cell wall fragments is more easily discernable in stereo images (Figs. 6, 7). In confocal projections the tracheid walls have a compressed appearance and there are no identifiable features such at pits or lumens apparently because of the compression and overall damage to the tracheid cell walls (Fig. 6a). Stereo images using FESEM allow visualisation of the fibrous texture over relatively wide areas and give a clear perspective of the torn tracheids protruding from the surface (Fig. 6b).

Stereoscopic imaging of the projected serial section sequences reveals a useful depth perspective, clearly showing twisting of tracheid bundles and shredding of cell walls at their surface (Fig. 7). This type of 3D imaging provides more detailed information on the internal structure of the sawn surface revealing details that were not obvious in confocal or scanning electron micrographs. For example it is possible to discern pits and tears in the cell walls well below the outer surface of the saw cut that are not obvious in 2D projections (Fig. 7).

Discussion

Cell wall deformation from sawing

Our results based on scanning electron microscopy and confocal microscopy are similar to those reported earlier by Nordström and Johansson (1995). They describe the sawn surface of spruce as being ‘‘very deformed or demolished’’ to depths of 1–200 μm. However, by using serial sectioning we have confirmed that the damaged region may extend beyond 600 μm. In addition, serial sectioning shows more details of the internal structure not visible in the surface images provided by confocal

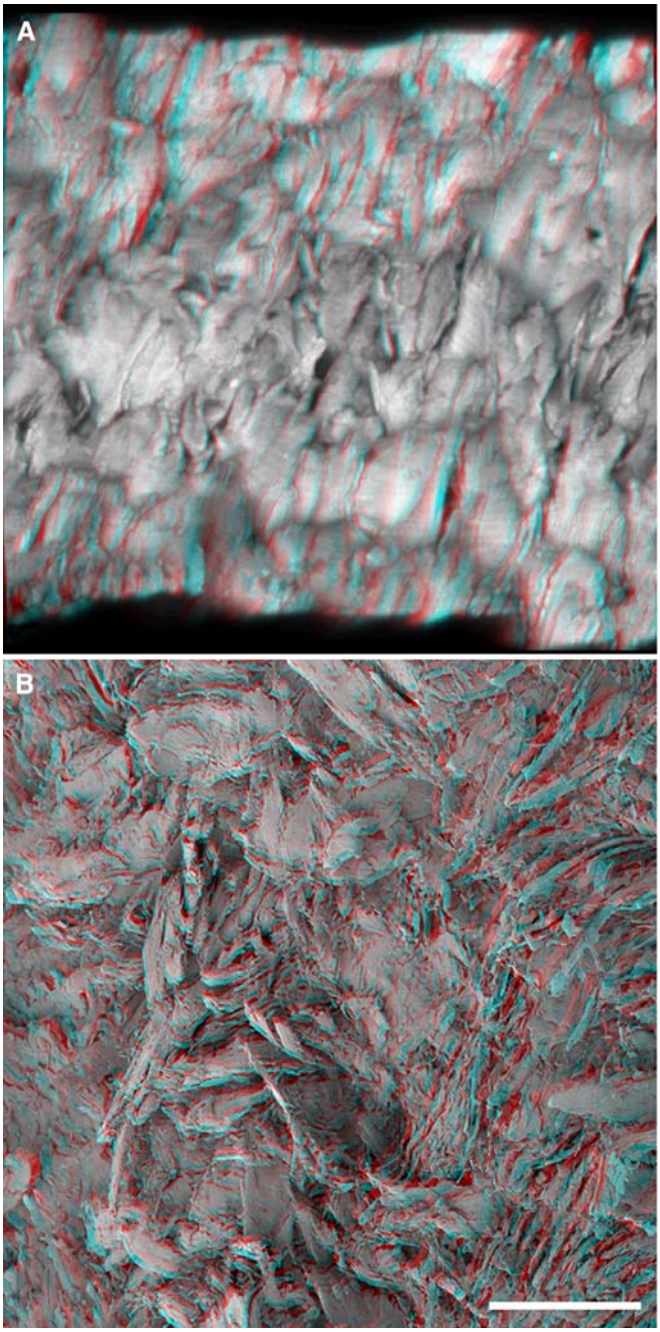

Fig. 6 **a** A maximum intensity anaglyph projection based on confocal microscopy. Field of view 625×625 μm. **b** A stereo image based on scanning electron microscopy. When viewed with red/green or red/blue glasses, these images can be seen in stereo with depth perspective. Glasses should be used with the red filter to the right eye. *Scale bar* 100 μm

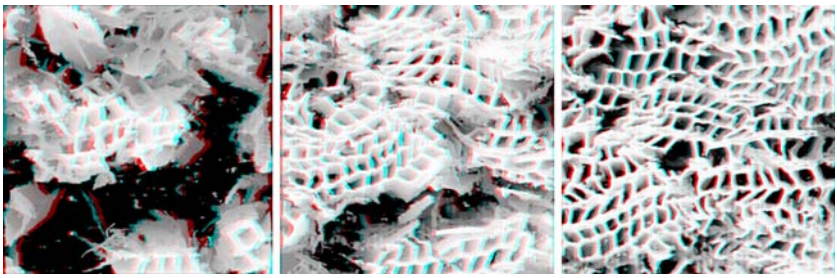

Fig. 7 Depth shaded anaglyph projections based on light microscopy of serial sections showing successive depths below the sawn surface 0–300, 300–500 and 500–635 μm from *left* to *right*. When viewed with red/green or red/blue glasses, these images can be seen in stereo with depth perspective. Glasses should be used with the red filter to the right eye. Field of view 625 × 625 μm

microscopy or electron microscopy. Confocal microscopy has the potential to provide a much faster and easier method for viewing this internal structure but we found that because of the dense surface, information about the underlying distortion is limited by light absorption. In addition confocal microscopy is limited to about 120 μm of depth because of the working distance of the objective lens (Donaldson and Lausberg 1998). It may be possible to examine the internal structure by microtoming part of the surface but such sectioning may result in modification of the distortion induced by sawing so we did not investigate this approach.

We have used stereo imaging to visualise the surface roughness of the sawn surface. We are unaware of other investigations using this approach to examine machined surfaces. Donaldson and Bond (2005) provide stereo images of wood structure based on confocal microscopy. Using the same method for scanning electron microscopy offers the advantage of higher resolution, greater depth of field or wider field of view than that available by confocal microscopy, and thus provides a useful method for evaluation of surface roughness on the sawn surface.

The deformation at the sawn surface and within the damaged region below the surface combines crushing and tearing involving both trans- and intra-wall fracture. Using serial sectioning, we have demonstrated that not all tracheids are deformed to the same extent, with tracheids forming groups that are severely damaged on the perimeter but only slightly deformed in the interior. This effect is not visible by surface imaging using electron microscopy or confocal microscopy. As discussed by Nordström and Johansson (1995), the depth of damage at the surface will influence the strength of adhesive bonds and the ability of the surface to accept coatings. The roughness of a machined surface affects its ability to accept coatings by influencing the distribution and penetration of coating films (de Meijer et al. 1998; Singh and Dawson 2006). Film thickness is influenced by the surface structure and is greatest in the grooves and thinnest over the ridges (Singh and Dawson 2006).

Three-dimensional reconstruction

Three-dimensional reconstruction using either physical serial sections or confocal optical sections can produce virtual models of wood or fibre structure (Bardage

2001; Bardage et al. 2002; Aronsson 2002; Chinga et al. 2004; Donaldson and Bond 2005). Such models can be represented as projections with perspective view (Aronsson 2002; Chinga et al. 2004; Donaldson and Bond 2005), as animations (Donaldson and Bond 2005) or as interactive objects suitable for display on web pages (Bardage 2001). The advantage over conventional 3D images provided by scanning electron microscopy for example (Core et al. 1979; Butterfield and Meylan 1980), is the ability to view from any orientation and to digitally cut away parts of the structure to reveal internal details. In our investigation of sawn surfaces we have demonstrated the usefulness of 3D reconstruction in understanding the complex internal structure of the sawn surface. This technique may also be useful for other investigations of machined wood surfaces, decayed or weathered wood and for wood anatomical investigations (Bardage 2001; Bardage et al. 2002).

Serial sectioning is difficult compared to optical sectioning by confocal microscopy because of the need for alignment of individual images, but has the advantage of much greater imaging depth, which is quite limited in confocal imaging by light absorption and by the working distance of the objective lens. Software algorithms for automated alignment are available and such tools could improve the processing of image sequences. For our investigation we used partially automated alignment followed by manual fine-tuning in order to optimise the image sequence. Sections of embedded wood do distort to a slight extent when dried on to the microscope slide and some method for removing this distortion could further improve the quality of alignment. Aronsson (2002) was able to perform translation, rotation, scale and shear corrections during alignment. Because of the relatively intensive sampling used (2 μm intervals) we were able to align images using recognisable features between adjacent images in the sequence. Bardage (2001) was also able to align serial sections using reference points such as ring boundaries, rays and neighbouring tracheids. Other attempts at serial sectioning have used fiducial marks in the form of plastic beads (Chinga et al. 2004).

For projection of sawn surface images we used only the original image sequence without interpolation between adjacent images. Again because of the intensive sampling at 2 μm intervals interpolation seemed unnecessary. We did however manually edit the image sequence to remove any objects that were present in only a single section. These objects were typically defects in the sections such as holes or stain deposits. Both Bardage (2001) and Chinga et al. (2004) used SEM images produced either by serial sectioning or by serial grinding which may have been free from such artefacts. These methods also largely avoid the distortion caused by stretching of thin sections. Chinga et al. (2004) used a 5 μm sampling interval and found it necessary to interpolate between images in the sequence, while Bardage et al. (2002) used 4 μm sections. The method based on vector imaging used by Bardage (2001) also incorporates some degree of smoothing of the rendered surface (Fig. 5). Although the vector based method has some advantages we found some problems with this method for use with the sawn surface data. Because the tracheids are damaged the cell wall surfaces may contain holes which cause rendering errors. We found that bitmap based projection methods are not affected in this way and are thus more suited to this application.

Conclusions

Using three different imaging methods, confocal microscopy, scanning electron microscopy, and light microscopy of serial sections combined with 3D reconstruction, we have illustrated both the external and interior structure of a sawn surface. The serial sectioning approach provides additional information on sub-surface deformation and damage compared to the two surface imaging methods, and may be suitable for investigating the structure of a range of machined wood surfaces and their interaction with adhesives and coatings. We have also demonstrated the usefulness of stereo imaging in visualising the texture of machined wood surfaces.

Acknowledgments This investigation was funded in part by a grant from the ISAT Linkages fund of the Royal Society of New Zealand for the authors' visit to Sweden from December 2001 to February 2002. This work was carried out within the framework of the Wood Ultrastructure Research Centre (WURC), a competence centre at the Swedish University of Agricultural Sciences. The authors are grateful to Adya Singh and Bernard Dawson, Ensis, Rotorua, for their helpful comments on the manuscript.

References

Aronsson M (2002) On 3D fibre measurements of digitised paper: from microscopy to fibre network. Silvestria 254, Swedish University of Agricultural Sciences, Uppsala, pp 1–72

Bardage SL (2001) Three-dimensional modelling and visualisation of whole Norway spruce latewood tracheids. Wood Fiber Sci 33:627–638

Bardage SL, Daniel G, Singh A (2002) Three-dimensional analysis of the collapse behaviour of Kraft-cooked Norway spruce fibres. Wood Fiber Sci 34:382–390

Bassett KH (1960) Effect of certain variables on strength of glued end joints. Forest Prod J 10:579–585

Butterfield BG, Meylan BA (1980) The three-dimensional structure of wood: an ultrastructural approach. Chapman and Hall, London

Chinga G, Johnsen PO, Diserud O (2004) Controlled serial grinding for high-resolution three-dimensional reconstruction. J Microsc 214:13–21

Core HA, Day AC, Côté WA (1979) Wood structure and identification. Syracuse wood science series 6, 2nd edn. Syracuse University Press, Syracuse

Donaldson LA, Bond J (2005) Fluorescence microscopy of wood. Scion, Rotorua, (CD-ROM)

Donaldson LA, Lausberg MJF (1998) Comparison of conventional transmitted light and confocal microscopy for measuring wood cell dimensions by image analysis. IAWA J 19:321–336

Hernández RE, Rojas G (2002) Effects of knife jointing and wear on the planed surface quality of sugar maple wood. Wood Fiber Sci 34:293–305

Jang HF, Robertson AG, Seth RS (1991) Optical sectioning of pulp fibers using confocal scanning laser microscopy. Tappi J 74:217–219

Jang HF, Amiri R, Seth RS, Karnis A (1995) Fiber characterization using confocal microscopy – collapse behaviour of mechanical pulp fibers. Tappi J 79:203–221

Kitin PB, Sano Y, Funada R (2003) Three-dimensional imaging and analysis of differentiating secondary xylem by confocal microscopy. IAWA J 24:211–222

Liptakova E, Kudela J, Bastl Z, Spironova I (1995) Influence of mechanical surface treatment of wood on the wetting process. Holzforschung 49:369–375

Marian JE, Stumbo DA, Maxey CW (1958) Surface texture of wood as related to glue-joint strength. Forest Prod J 8:345–351

de Meijer M, Thurich K, Militz H (1998) Comparative study on penetration characteristics of modern wood coatings. Wood Sci Technol 32:347–365

Moëll M, Donaldson LA (2001) Comparison of segmentation methods for digital image analysis of confocal microscope images to measure tracheid cell dimensions. IAWA J 22:267–288

Möller R, McDonald AG, Walter C, Harris PJ (2003) Cell differentiation, secondary cell-wall formation and transformation of callus tissue of *Pinus radiata* D. Don. Planta 217(5):736–747

de Moura LF, Hernández RE (2005) Evaluation of varnish coating performance for two surfacing methods on sugar maple wood. Wood Fiber Sci 37:355–366

de Moura LF, Hernández RE (2006) Effects of abrasive mineral, grit size and feed speed on the quality of sanded surfaces of sugar maple wood. Wood Sci Technol 40:517–530

Murmanis L, River BH, Stewart HA (1986) Surface and subsurface characteristics related to abrasive-planing conditions. Wood Fiber Sci 18:107–117

Nordström JEP (1995) Bending strength of spruce end-grain butt-joints using resorcinol formaldehyde-based adhesives. Forest Prod J 45:77–83

Nordström JEP, Johansson I (1995) End-grain glue-joint strength. Part 2: The microstructure of machined end-grain surfaces of spruce timber. Holz Roh- Werkst 53:38

Quirk JT, Kozlowski TT, Blomquist RF (1967) Location of failure in adhesive bonded butt joints. Note FPL 0177, USDA Forest Service, Forest Products Laboratory, Madison

Singh AP, Dawson BSW (2006) Microscopic assessment of the effect of saw-textured *Pinus radiata* plywood surface on the distribution of a film-forming acrylic stain. JCT Res 3:193–201

Stehr M, Östlund S (2000) An investigation of the crack tendency on wood surfaces after different machining operations. Holzforschung 54:427–436

Stewart HA, Crist JB (1982) SEM examination of subsurface damage of wood after abrasive and knife planing. Wood Sci 14:106–109

Suchsland O (1958) Über das Eindringen des Leimes bei der Holzverleimung und die Bedeutung der Eindringtiefe für die Fugenfestigkeit. Holz Roh-Werkst 16:101–108

Vazquez-Cooz I, Meyer RW (2006) Cutting forces for tension and normal wood of maple. Forest Prod J 56:26–34

Wu R (1998) Microstructural study of sanded and polished wood by replication Wood Sci Technol 32:247–260